International Research Journal of Pure & Applied Chemistry

21(18): 33-42, 2020; Article no.IRJPAC.62169
ISSN: 2231-3443, NLM ID: 101647669

Characterization of Cellulose Nanocrystals Derived from Umbrella Plant (*Cyperus alternifolius* Linn.)

Marcelino R. Tradio Jr.[1*] and Brian John Sarno[1]

[1]Department of Chemistry, University of San Carlos, Talamban, Cebu City, 6000, Philippines.

Authors' contributions

This work was carried out in collaboration between both authors. Author MRTJ designed the study, wrote the protocol, managed the literature search, performed the analyses and wrote the first draft of the manuscript. Author BJS supervised the analyses of the study and proof read the first draft of the manuscript. Both authors read and approved the final manuscript.

Article Information

DOI: 10.9734/IRJPAC/2020/v21i1830269
Editor(s):
(1) Dr. Richard Sawadogo, Research Institute for Health Sciences, Burkina Faso.
Reviewers:
(1) M. Ravichandran, K. Ramakrishnan College of Engineering (Affiliated to Anna University), India.
(2) M. V. Praveen Kumar, India.
(3) M. Rudresh, Dayananda Sagar College of Engineering, India.
Complete Peer review History: http://www.sdiarticle4.com/review-history/62169

Original Research Article

Received 04 August 2020
Accepted 10 October 2020
Published 17 October 2020

ABSTRACT

Plant–based nanocrystals have gained wide research interest due to its application in nano–reinforcement. Hence, the study investigated the stems of umbrella plant as potentials source of cellulose fibers to synthesize cellulose nanocrystals (CNCs). The synthesis of CNCs were conducted using acid hydrolysis with 10 mL 64% w/w sulfuric acid for each gram of purified cellulose at 45°C for 30 min. The surface morphology, structural, physical and thermal properties of CNCs were characterized using field emission scanning electron microscopy (FESEM), transmission electron microscopy (TEM), Fourier Transform Infrared spectroscopy (FTIR), X–ray diffractometer (XRD), and simultaneous thermal analyzer, respectively. The result showed that the CNCs were mixture of rod–like shape and spherical morphology. The CNC rods were less than 20 nm width and 200–300 nm length when viewed under FESEM. However, the CNC rods were shorter when viewed under TEM and had a width less than 5 nm and length between 20–50 nm. The spherical CNCs that were seen only under TEM were less than 20 nm in diameter. The FTIR spectra showed that the CNCs were composed of crystalline cellulose I wherein the molecular structure of cellulose was preserved after the hydrolysis. The XRD patterns showed that the CNCs were highly crystalline with crystallinity index value of 94.48%. Lastly, the CNCs exhibited a three–stage thermal decomposition behavior.

**Corresponding author: E-mail: marsthebiochemist@gmail.com;*

Keywords: Umbrella plant; Cyperus alternifolius; cellulose nanocrystals.

1. INTRODUCTION

Synthesis of nanomaterials derived from cellulose have gained increasing interest due to their potential as nano–reinforcing fillers into biocomposites for industrial and biomedical applications [1]. Two general classes of cellulose nanomaterials include cellulose nanocrystals (CNCs) and cellulose nanofibrils. Cellulose nanocrystals—also known as cellulose nanowhiskers or nanocrystalline cellulose [2–3], cellulose crystallites, cellulose crystals, cellulose monocrystals and cellulose microcrystals [4–6] exhibit suitable characteristics for used as reinforcement that attract both research scientists and industrialists. The nanoparticles have abundant hydroxyl groups, large surface area, high aspect ratio (length to width ratio), high crystallinity, good mechanical properties, and high thermal stability [7–9]. They are synthesized from different natural sources including plants and animals [2–3]. However, plant–based cellulose has been used extensively for the production of CNCs [10].

Plant cellulose which appears as microfibril is surrounded with cementing matrix of polysaccharides and glycoproteins like lignin, hemicellulose and pectin [11] The assembly of helically cellular cellulose microfibrils embedded in the cementing material is formed from long–chain cellulose molecules [12].The elementary fibrils and nano–scale cellulose fiber units are formed from 30–100 individual cellulose molecules [13–14] through inter and intra molecular hydrogen bonding attributed from the three hydroxyl groups on each glucose unit of cellulose chain into hierarchical microstructures [15–16]. The strong and complex network of hydrogen bonds between cellulose molecules stabilize the arrangement of the cellulose chain into a highly ordered structure via crystalline packing that eventually form into slender and nearly endless crystalline rods along the microfibril axis [12,17–18]. Meanwhile, the disordered amorphous holocellulose segments which lack hydroxyl groups are bonded with cellulose crystals [19–20]. However, the amorphous regions can be hydrolyzed by strong acid treatment of cellulose microfibril, leaving behind the highly crystalline residue, known as CNCs [21].

Though the synthesis of CNCs has been conducted extensively in details from variety of natural plant fibers, the use of stems from umbrella plant has not been investigated. Umbrella plant—commonly known as umbrella papyrus, umbrella sedge or umbrella palm—is a grass–like perennial sedge plant in the very large genus Cyperus of the sedge family, Cyperaceae. It is native to Madagascar but is frequently cultivated worldwide as an ornamental or pot plants. It is cultivated as a fiber plant or ornamental in South–East Asia and elsewhere in the tropics. It grows to 3–5 ft along edges of streams, ponds, and lakes, where water is plenty. The flowers, which occur in clusters of 10–20, are brownish spadix produced in the center of the leaves [22]. The plant has strong underground root and erect aerial stem, which does not have any branches [23].

In the Philippines, the stems are used for mat–making. The stems produce 50% or more when pulp at 100°C and atmospheric pressure. The strength of unbeaten pulp was similar to that of beaten softwood pulps, but drainage was very slow. A strong paper was obtained by blending with unbeaten wood pulps [24].

The present study aims to synthesize the CNCs from the purified cellulose fiber of umbrella plant and characterize their selected properties using Field Emission Scanning Electron Microscopy (FESEM), Transmission Electron Microscopy (TEM), Fourier Transform Infrared (FTIR Spectroscopy, X–ray Diffraction (XRD), and thermal analyzer. The results of the study could be used as benchmark in considering the newly synthesized CNCs as reinforcement agents for nanocomposite preparation.

2. MATERIALS AND METHODS

2.1 Materials

The umbrella plant stems were collected from the Butuanon Riverbank located at Budlaan, Talamban Cebu City, Philippines. The chemical reagents used in the entire preparation of cellulose fiber and synthesis of CNCs were analytical grade without further purification.

2.2 Extraction and Purification of Cellulose Fiber

The crude fiber was extracted using water–retting process [25]. Briefly, the long and continuous stems were cut into pieces having approximate length of 30 cm each and kept immersed in water for 2 weeks. During this period, the stems were softened and degraded due to the presence of microorganisms in water. Then, the fibers were separated from the stem piths and washed thoroughly with double–distilled water to remove their impurities. The obtained fibers were air–dried for 48 h to remove the moisture. The extracted fibers underwent purification.

The purification of cellulose fiber involved alkali and bleaching treatment [26]. The *C. alternifolius* fibers were treated with 5% w/w aqueous solution of sodium hydroxide for 30 min at 30°C maintaining a liquor ratio of 30:1. The fibers were washed several times with water to remove all traces of NaOH from the fiber surface. The washed fibers were dried in a hot air oven at 105 °C for 8 h. Then, the alkali–treated fibers were milled using Thomas–Wiley Laboratory Mill to pass through a 60–mesh size screen. The sieved fibers were dewaxed by refluxing with toluene–ethanol (2:1, v/v) for 6 h in a Soxhlet apparatus. The dewaxed fibers were bleached with a solution made up of equal parts (v/v) of acetate buffer (27 g NaOH and 75 mL glacial acetic acid diluted to 1 L of distilled water) and aqueous sodium chlorite (1.7% w/v $NaClO_2$ in water) using a fiber/liquor ratio of 1:50. The bleaching treatment was performed at 80°C for 4 h. The mixture was filtered and extensively washed with 2% w/v sodium bisulfite, distilled water, and 95% v/v ethanol. The residues were dried at 105°C in an oven for 8 h until constant weight. The crude holocelluloses were treated with 17.5% w/v sodium hydroxide solution at 30°C for 45 min. The treated fibers were washed with distilled water and 95% v/v ethanol to neutralize the reaction. Finally, the purified cellulose fibers were dried at 105 °C in an oven for 8 h until constant weight and stored in air tight polybags.

2.3 Synthesis of the Cellulose Nanocrystals

The synthesis of CNCs from purified cellulose fibers of umbrella plant utilized a well–established acid hydrolysis [27]. The hydrolysis was performed at 45 °C under magnetic stirring using a pre–heated 64% w/w sulfuric acid for 30 min. For each gram of purified cellulose, 10 mL of pre–heated 6.5 M H_2SO_4 was added to the sample. Heating was done using a temperature–controlled water bath. The mixture was allowed to hydrolyze under vigorous stirring. Immediately after the hydrolysis, the suspension was diluted with 10–fold cold water to stop the hydrolysis reaction, and was allowed to settle overnight. The clear top layer was decanted and the remaining white cloudy layer was centrifuged for 10 min at 6000 rpm. The suspension was washed and centrifuged repeatedly for three times. The thick white suspension after the last centrifugation was placed inside a Fisherbrand regenerated cellulose dialysis membrane tubes (12–14 kDa molecular weight cut off) and dialyzed against Milli Q ultrapure water for seven days. The dialysis was continued until such the membrane tube containing the CNCs was placed periodically in water, the pH of the water become neutral over a period of 1 h. Subsequently, the suspension was sonicated for 10 min to disperse the particles homogeneously. The aqueous suspension was dried using a FT–10–R vacuum freeze dryer (Labfreeze Instruments Co. Ltd).

2.4 Characterization of Cellulose Nanocrystals

2.4.1 Morphology

The morphologies of untreated fibers, purified cellulose fibers, and CNCs were examined using Zeiss Supra 55VP Field Emission Scanning Electron Microscope (Germany) of USC–Physics Department Material Science Division with an accelerating voltage of 1.5 kV. The dried samples were placed on a sample holder and sputtered-coated with gold to avoid the charging effect. The samples were visualized at various magnifications.

For transmission electron microscopy (TEM), the only the CNCs were examined using JEM–2100F transmission electron microscope (JEOL, Japan) at the Advanced Material Technology Laboratory of the Department of Science and Technology. The freeze–dried cellulose nanocrystals were re–dispersed into ethanol. A drop of 10 uL about 0.005% w/v cellulose nanocrystals suspension was added onto the carbon–coated electron microscopy grid and the excess liquid was absorbed by a filter paper. The specimens were then negatively stained with 2% uranyl acetate. Excess solution was blotted out with a filter paper and allowed to dry by evaporation at ambient condition. The sample grid was observed at 200 kV.

2.4.2 Fourier transform infrared (FTIR) spectroscopic analysis

The FTIR spectra of untreated fibers, purified cellulose fibers, and CNCs were recorded at room temperature using Perkin Elmer FT_{100} Fourier–Transform Spectrometer of University of San Carlos (USC)–Chemistry Department. The dried samples were analyzed in transmittance mode within the range of 4000–600 cm^{-1} at a resolution of 4 cm^{-1} using attenuated total reflectance (ATR) technique of the FTIR instrument.

2.4.3 X–ray diffraction analysis

The physical analyses were evaluated through X–ray diffraction (XRD) using Shimadzu Lab–X XRD–6000 X–ray diffractometer at Materials Science Division of the Department of Science and Technology. The experiment was performed with a scanning rate of 1° per min with Cu Kα radiation source (λ 1.5418 Å) operating at 40 kV and 30 mA. The XRD patterns were obtained over the angular range 2θ 2–60°. The crystallinity indices of the samples were calculated using Segal method as shown in the equation below.

$$CrI = [(I_{002} - I_{\mathrm{am}}) \div I_{002}] \times 100$$

In this equation, *CrI* expresses the relative degree of crystallinity, I_{002} is the intensity of the 002 lattice diffraction at 2θ 22.8°, and I_{am} is the intensity of diffraction at 2θ 18.0°. I_{002} represents both crystalline and amorphous regions while I_{am} represents only the amorphous component.

2.4.4 Thermal analysis

The thermal properties were determined using Perkins Elmer STA 6000 simultaneous thermal analyzer at Advanced Device and Materials Testing Laboratory of the Department of Science and Technology. The runs were performed at heating rates of 10 °C/min from 30°C to 995°C under high purity nitrogen at a flow rate of 50 mL/min. A 10 mg of sample was placed in a ceramic crucible holder.

3. RESULTS AND DISCUSSION

3.1 Morphology

Fig. 1 showed the FESEM micrographs of untreated fiber (A), purified cellulose (B) and CNCs (C); and TEM micrograph of CNCs (D). The untreated fiber appeared as bundles of fibers packed with massive cementing materials. However, during alkali and bleaching treatment, these cementing materials were removed as shown in the image of purified cellulose with smooth morphology. Cellulose microfibrils were also visible in the purified cellulose fibers. Meanwhile, sulfuric acid hydrolysis of the purified cellulose fiber at 45°C for 30 min produced two different types of nanocrystals, such as rod–like and spherical CNCs. The most abundant type was rod–like CNCs while the least was spherical. The image of the CNC rods in Fig. 1C were less than 20 nm width and between 200 and 300 nm length. However, the CNC rods were shorter when viewed using TEM (Fig. 1D). They were less than 5 nm width and between 20 and 50 nm length. It appeared that agglomeration of CNC rods occurred forming into larger bundles. Hence, the CNC rods were larger when viewed using FESEM. The formation of larger CNC rods could not be avoided because the samples were freeze–dried prior to FESEM analysis which increased the chance of intermolecular interactions. However, these bundles of CNC rods are well dispersed easily in ethanol during the preparation of TEM sample prior to their analysis. Hence, the much smaller CNC rods were observed under TEM.

Meanwhile, the spherical CNCs were identified using TEM with a diameter of less than 20 nm. The formation of spherical CNCs was due to the self–assembling of short CNC rods through interfacial hydrogen bonds. However, this interaction didn't exist to longer CNC rods. Hence, the spherical CNCs were not be visible using FESEM because the nanoparticles were relatively long. The identification of spherical CNCs from umbrella plant was additional library to very few sources of this type of CNCs, which were first identified in cellulose fibers of cotton [28].

3.2 FTIR Spectroscopic Analysis

The FTIR spectra presented in Fig. 2 showed the changes in chemical composition due to the chemical treatment of untreated umbrella fibers and sulfuric acid hydrolysis of purified cellulose. The peaks at 3393 cm^{-1} and between 2900–2800 cm^{-1} in the three spectra were attributed to the O–H stretching and C–H stretching of the cellulose [29–30]. The prominent peaks around 1600–1400 cm^{-1} and the peak at 1250 cm^{-1} in the spectrum of untreated fiber ascribed to the aromatic C=C stretch and C–O out of plane stretch [29], respectively, which were due to the aryl group of lignin [31]. These peaks decreased

in the spectrum of purified cellulose due to the removal of lignin, and disappeared in the spectrum of cellulose nanocrystals because of acid hydrolysis [32–33]. The other peaks at 1638, 1347, and 1033 cm^{-1} which appeared in all of the spectra are associated with the O–H bending, C–H bending; and stretching vibration of C–O–C pyranose β–1–4–glycosidic bond, a type of acetal linkage [18,29], respectively. A strong spectral band of C–H at 1347 cm^{-1} implied that the CNCs were composed of crystalline cellulose I [34–35]. Meanwhile, the decrease in the intensity of the peak at 1033 cm^{-1} for C–O–C pyranose glycosidic linkage confirmed the removal of amorphous region of the cellulose [36].

The differences of the spectra between untreated umbrella fiber and cellulose nanocrystals implied that the cellulose nanocrystals were produced after sulfuric acid hydrolysis of purified cellulose fiber from umbrella plant [37]. Meanwhile, no large significant differences were observed between the spectra of purified cellulose and cellulose nanocrystals which implied that the molecular structure of cellulose was preserved during acid hydrolytic process [32,37].

3.3 X–ray Diffraction Analysis

Fig. 3 showed the XRD patterns of the untreated fibers, purified cellulose fiber and CNCs which were predominantly a type I or native cellulose because of the presence of peaks at around 2Θ=18°, 2Θ=22.8°, and 2Θ=35°. It was observed that the main diffraction peak located at 2Θ=22.8° for CNCs was larger and sharper than the untreated fiber and purified cellulose. The result was an indicative that the CNCs had better defined crystalline domains which was confirmed further based from the value of crystallinity indices of the three materials. The crystallinity indices for the untreated fiber, purified cellulose and CNCs were 80.56, 87.40, and 94.48%, respectively. A much higher crystallinity of CNCs was attributed to the removal of amorphous components such as hemicellulose and lignin; and other non cellulosic components during bleaching and hydrolysis. The synthesis procedure resulted to the realignment of cellulose molecules and the release of individual crystallites [38]. Meanwhile, the broadening of the diffraction peaks at 2Θ=18° for untreated fiber, purified cellulose, and CNCs was due to the overlapping with peaks around 2Θ=15°.

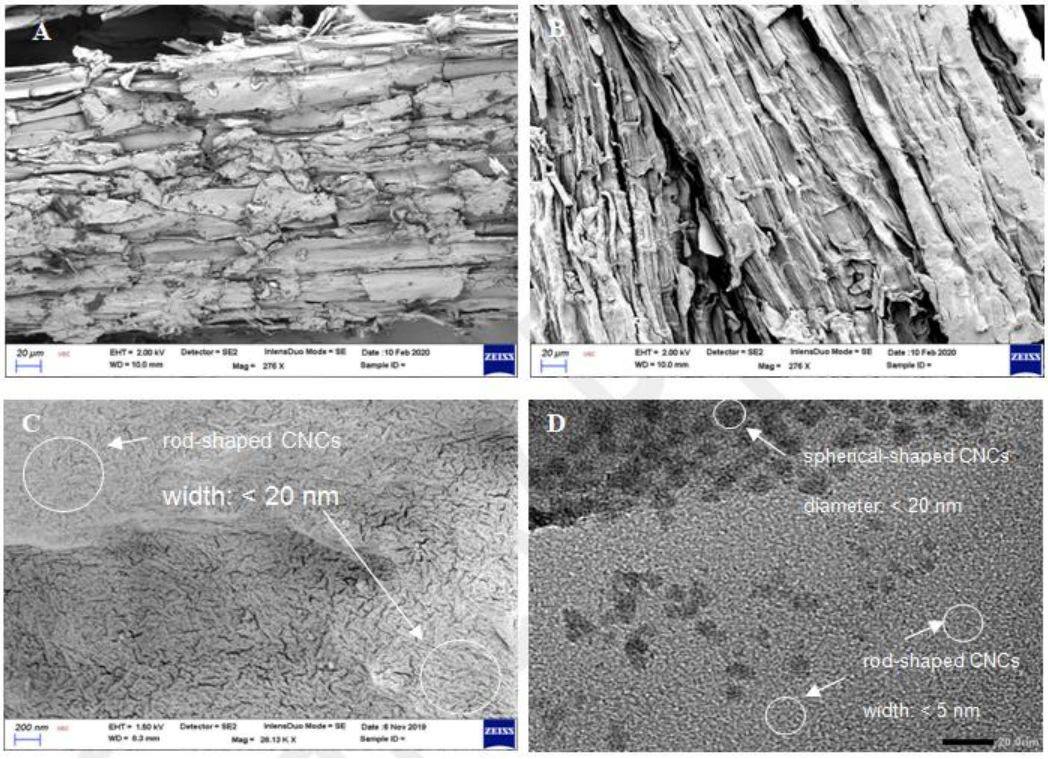

Fig. 1. FESEM micrographs of untreated fiber (A), purified cellulose fiber (B), and CNCs (C); and TEM micrograph of CNCs (D)

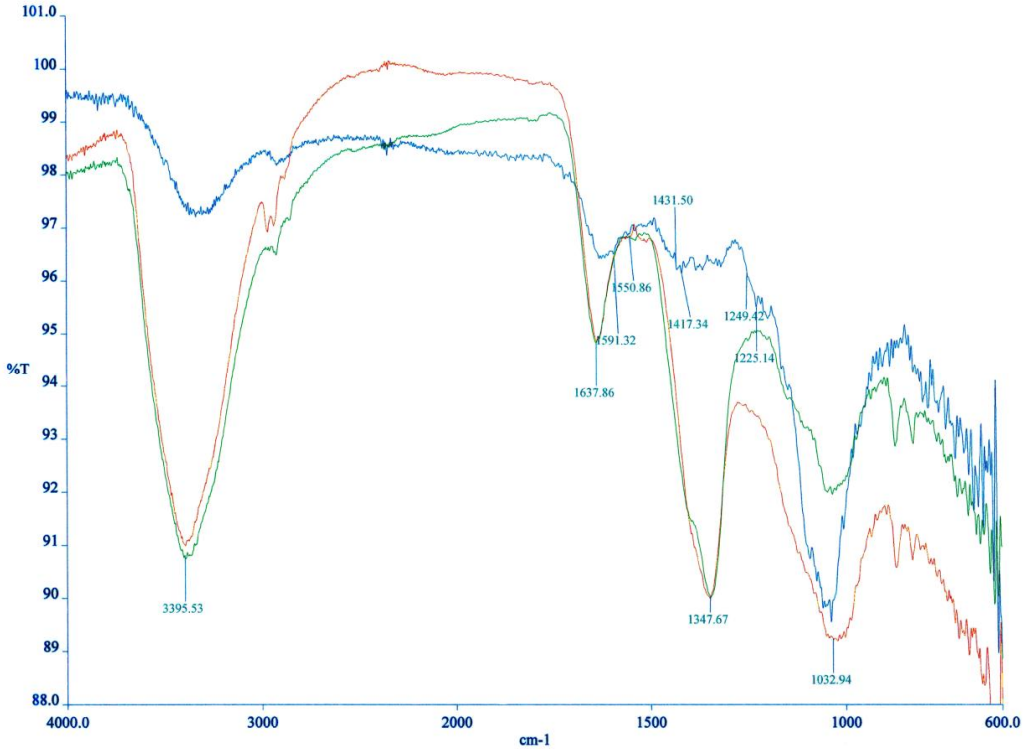

Fig. 2. FTIR spectra of untreated fiber (blue), purified cellulose fiber (red), and CNCs (green)

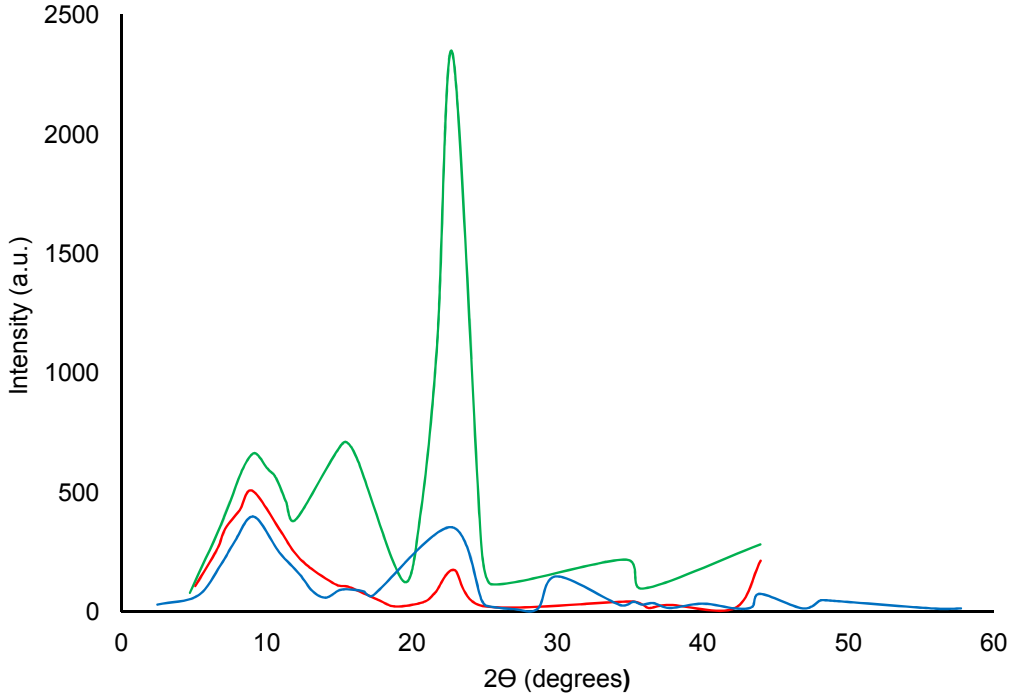

Fig. 3. XRD patterns of untreated fiber (blue), purified cellulose fiber (red), and CNCs (green)

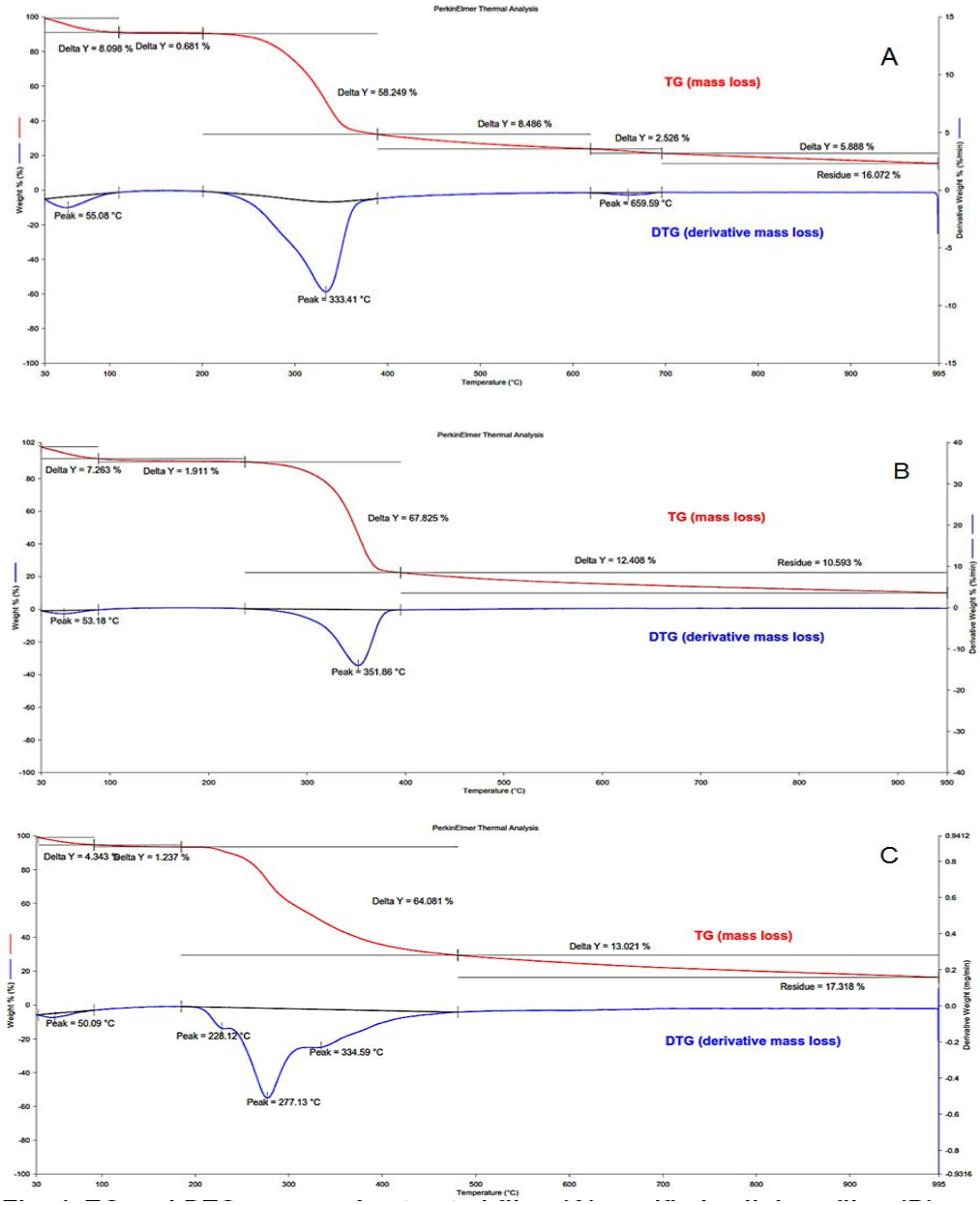

Fig. 4. TG and DTG curves of untreated fiber (A), purified cellulose fiber (B), and CNCs (C)

3.4 Thermal Analysis

Fig. 4 showed the thermogravimetric (TG) and derivative thermogravimetric (DTG) curves of untreated fiber, purified cellulose fiber and CNCs of umbrella plant. The three materials exhibited an initial decomposition at temperature peak between 50–55°C which corresponded to the evaporation of surface–bound moisture. The purified cellulose fiber exhibited a highest main decomposition temperature at 351.86°C which was ascribed to the weight loss of cellulose. Meanwhile, the untreated fiber showed the main decomposition at 333.41°C which was attributed to the pyrolysis of cellulose. A small broadening on the left of the main peak was observed which was due to the low decomposition temperature of hemicellulose, lignin and pectin; while a shoulder peak at 659.59°C was associated to higher char formation of non–cellulose components [31–32,35,37]. However, the CNCs exhibited a different decomposition behavior. A lower start

decomposition temperature was detected at 228.12°C. Then, a shoulder peak at 334.59°C was recorded after the main decomposition peak of 277.13°C. The decomposition temperatures at 228.12°C and 277.13°C were due to the degradation of sulfated regions; whereas, the high temperature decomposition was related to the breakdown of unsulfated regions of the CNCs [32,37].

The purified cellulose fibers had higher degradation temperature than the untreated fiber because the cellulose fibers underwent series of processes such as dehydration, depolarization and decomposition of glycosyl units before charred residues were formed. In addition, purified cellulose had lesser content or absence of non–cellulosic segments such as lignin and hemicelluloses which decomposed at lower temperature. Meanwhile, the CNCs had lower degradation temperature—an indicative of a lower thermal stability—because of their nano–sizes, greater number of free ends along the chain, drastic reduction in the molecular weight and degradation of highly–sulfated regions [39]. Moreover, the TG curve of CNCs was a three well–separated pyrolysis process [40]. The first two well–separated pyrolysis process are at 220–270°C, 270–330°C, and 330–470°C, respectively [41]; and a maximum temperature peak at a lower temperature (around 400°C) than the degradation of native cellulose [42]. The reduction of thermal stability of CNCs was due to the presence of sulfate group attached to the sugar units [43], which could be removed at a much lesser energy [44]. Specifically, the lower temperature stage was attributed to the degradation of more accessible highly sulfated regions, whereas the higher temperature stage was brought about by the breakdown of unsulfated crystal interior of CNCs [45].

4. CONCLUSION

The study showed that the purified cellulose fibers derived from the stems of umbrella plant were potential natural source of cellulose nanocrystals. Morphologically, the newly synthesized CNCs were mixed of both rod–like and spherical–shaped nanocrystals. The CNC rods were less than 20 nm width and 200–300 nm length when viewed under FESEM. However, the CNC rods appeared shorter when observed under TEM, which were less than 5 nm width and 20–50 nm length. Meanwhile, the spherical CNCs were obtained from the cellulose fibers of the plant that had a diameter of 20 nm approximately. Moreover, the CNCs were highly crystalline; yet, they were relatively had low thermal stability.

ACKNOWLEDGEMENTS

Author MRTJ expressed his gratitude to the Science Education Institute of the Department of Science and Technology, Republic of the Philippines for the funding aid in the form of a scholarship grant.

COMPETING INTERESTS

Authors have declared that no competing interests exist.

REFERENCES

1. Faruka O, Bledzki AK, Fink HP, Sain M. Biocomposites reinforced with natural fibers: 2000-2010. Prog. Polym. Sci. 2012; 37:1552-1596.
2. Fortunati E, Puglia D, Monti M, Peponi L, Santulli C, Kenny JM, Torre L. Extraction of cellulose nanocrystals from *Phormium tenax* Fibres. J. Polym. Environ. 2013;21: 319–328.
3. Siqueira G, Tapin–Lingua S, Bras J, da Silva Perez D, Dufresne A. Mechanical properties of natural rubber nanocomposites reinforced with cellulosic nanoparticles obtained from combined mechanical shearing, and enzymatic and acid hydrolysis of sisal fibers. Cellulose. 2010;18:57–65.
4. Peng BL, Dhar N, Liu HL, Tam KC. Chemistry and applications of nanocrystalline cellulose and its derivatives: A nanotechnology perspective. The Canadian Journal of Chemical Engineering. 2011;89:1191–1206.
5. Shi J, Shi SQ, Barnes HM. A chemical process for preparing cellulosic fibers hierarchically from kenaf bast fibers. Biores. 2011;6:879–90.
6. Lima MMS, Borsali R. Rodlike cellulose microcrystals: structure, properties, and applications. Macromol. Rapid Commun. 2004;25:771–787.
7. Silvério HA, Neto WPF, Dantas NO. Extraction and characterization of cellulose nanocrystals from corncob for application as reinforcing agent in nanocomposites. Ind Crops Prod. 2013;44:427–36.
8. Islam MT, Alam MM, Zoccola M. Review on modification of nanocellulose for

application in composites. Int J Innovative Research in Sci, Engand Technol. 2013;2: 5444–5451.
9. Zhang W, Yang XL, Li CY. Mechanochemical activation of cellulose and its thermoplastic polyvinyl alcohol ecocomposites with enhanced physicochemical properties. Carbohyd Polym. 2011;83:257–263.
10. Eichhorn SJ, Dufresne A, Aranguren M, Marcovich NE, Capadona JR, Rowan SJ, et al. Review: Current international research into cellulose nanofibres and nanocomposites. J. Mater. Sci. 2010;45:1-33.
11. Khalil HPSA, Davoudpour Y, Islama MN. Production and modification of nanofibrillated cellulose using various mechanical processes: A review. Carbohyd Polym. 2014;99:649–65.
12. Kalia S, Dufresne A, Cherian BM. Cellulose-based bio- and nanocomposites: A review. Int J Polym Sci. 2011;1-35.
13. Lavoine N, Desloges I, Dufresne A, Bras J. Microfibrillated cellulose–Its barrier properties and applications in cellulosic materials: A review. Carbohydr. Polym. 2012;90:735–764.
14. Wang B, Sain M, Oksman K. Study of structural morphology of hemp fiber from the micro to the nanoscale. Applied Composite Materials. 2007;14;89–103.
15. Reddy MM, Vivekanandhan S, Misra M. Biobased plastics and bionanocomposites: Current status and future opportunities. Prog. Polym. Sci. 2013;38:1653–1689.
16. Liu HY, Liu D, Yao F. Fabrication and properties of transparent polymethyl methacrylate/cellulose nanocrystals composites. Biores Technol. 2010;101: 5685–92.
17. Frone AN, Panaitescu DM, Donescu D. Preparation and characterization of PVA composites with cellulose nanofibers obtained by ultrasonication. Biores. 2011; 6:487–512.
18. Alemdar A, Sain M. Isolation and characterization of nanofibers from agriculturalresidues–wheat straw and soy hulls. Bioresour. Technol. 2008;99:1664–1671.
19. Tonoli GHD, Teixeira EM, Corrêa AC. Cellulose micro/nanofibres from Eucalyptus kraft pulp: Preparation and properties. Carbohyd. Polym. 2012;89:80–88.
20. Dalmas F, Chazeau L, Gauthier C. Large deformation mechanical behavior of flexible nanofiber filled polymer nanocomposites. Polym. 2006;47:2802–2812.
21. Floros M, Hojabri L, Abraham E. Enhancement of thermal stability, strength and extensibility of lipid-based polyurethanes with cellulose-based nanofibers. Polym Degrad and Stabil. 2012;97:1970-1978.
22. Ahmed AH. Chemical and Biological Studies of *Cyperus alternifolius* Flowers essential oil. Asian Journal of Chemistry. 2012;24:4768–4770.
23. Liao X, Luo S, Wu Y, Wang Z. Comparison of nutrient removal ability between *Cyprus alternifolius* and *Vetiveria zizanioides* in constructed wetlands. Chinese Journal of Applied Ecology. 2005;16:156–160.
24. Anonymous. PlantUse; 2016. Accessed 21 March 2018. Available:https://uses.plantnetproject.org/en/Cyperus_alternifolius_(PROSEA).
25. Natarajan T, Kumaravel A, Palanivelu R. Extraction and characterization of natural cellulosic fiber from *Passiflora foetida* stem. International Journal of Polymer Analysis and Characterization. 2016;21: 478–485.
26. Obi Reddy K, Ashok K, Raja Narender Reddy K, Feng YE, Zhang J, Varada Rajalu A. Extraction and characterization of novel lignocellulosic fibers from Thespesia lampas plant. Int. J. Polym. Anal Charact. 2016;19:48–61.
27. Hamad WY. Hydrolytic extraction of cellulose nanocrystals. Cellulose nanocrystals: Properties, production, and applications. John Wiley & Sons, Inc.: Chichester, West Sussex, United Kingdom; 2017.
28. Lu P, Hsieh YL. Preparation and properties of cellulose nanocrystals: Rods, spheres, and network. Carbohydrate Polymers. 2010;82:329–336.
29. Pavia DL, Lampman GM, Kriz GS, Vyvyan JR. Introduction to spectroscopy. 5th ed. Cengage Learning: 200 First Stamford Place, 4th Floor, Stamford, CT 06902, USA; 2015.
30. Sain M, Panthapulakkal S. Bioprocess preparation of wheat straw fibres and their characterization. Ind Crops Prod. 2006;2: 1–8.
31. Neto WPF, Silverio HA, Dantas NO, Pasquini D. Extraction and characterization

of cellulose nanocrystals from agro-industrial residue–Soy hulls. Industrial Crops and Products. 2013;42:480–488.
32. Li R, Fei J, Cai Y, Li Y, Feng J, Yao J. Cellulose whiskers extracted from mulberry: A novel biomass production. Carbohydrate Polymers. 2009;76:94–99.
33. Troedec M, Sedan D, Peyratout C, Bonnet J, Smith A, Guinebretiere R, Gloaguen V, Krausz P. Influence of various chemical treatment on the composition and structure of hemp fibres. Compos Part A. 2008;39: 514–522.
34. Kumar A, Lee Y, Kim D, Rao KM, Kim J, Park S, Haider A, Lee DH, Han SS. Effect of crosslinking functionality on microstructure, mechanical properties, and in vitro cytocompatibility of cellulose nanocrystals reinforced poly (vinyl alcohol)/ sodium alginate hybrid scaffolds. International Journal of Biological Macromolecules. 2016;1–11.
35. Kumar A, Negi YS, Choudhary V, Bhardwaj NK. Characterization of Cellulose nanocrystals produced by acid–hydrolysis from sugarcane bagasse as agro–waste. Journal of Materials Physics and Chemistry. 2014;2:1–8.
36. Wang LF, Shankar S, Rhim JW. Properties of alginate–based films reinforced with cellulose fibers and cellulose whiskers isolated from mulberry pulp. Food Hydrocolloids. 2017;63:201–208.
37. Kargarzadeh H, Ahmad I, Abdullah I, Dufresne A, Zainudin SY, Sheltami RM. Effects of hydrolysis conditions on the morphology, crystallinity, and thermal stability of cellulose nanocrystals extracted from kenaf bast fibers. Cellulose. 2012;19: 855–866.
38. de Souze Lima MM, Borsali R. Rodlike cellulose microcrystals: Structure, properties and applications. Macromolecular Rapid Communications. 2004;25: 771–787.
39. Mandal A, Chakrabarty D. Isolation of nanocellulose from waste sugarcane bagasse (SCB) and its characterization. Carbohydr. Polym. 2011;86:1291–1299.
40. Wang N, Ding EY, Chang RS. Thermal degradation behaviors of spherical cellulose nanocrystals with sulfate groups. Polymer. 2007;48:3486–3493.
41. Li W, Wang R, Liu S. Nanocrystalline cellulose prepared from softwood kraft pulp via ultrasonic-assisted acid hydrolysis. Bioresources. 2011;6:4271–4281.
42. George J, Sajeevkumar VA, Kumar R, Ramana KV, Sabapathy SN, Bawa AS. Enhancement of thermal stability associated with the chemical treatment of bacterial (*Gluconacetobacter xylinus*) cellulose. J. Appl. Polym. Sci. 2008;8: 1845–1851.
43. Maren R, William TW. Effect of sulfate groups from sulfuric acid hydrolysis on the thermal degradation behavior of bacterial cellulose. Biomacromolecules. 2004;5: 1671–1677.
44. Julien S, Chornet E, Overend RP. Influence of acid pre-treatment (H_2SO_4, HCl, HNO_3) on reaction selectivity in the vacuum pyrolysis of cellulose. Journal of Analytical and Applied Pyrolysis. 1993;27: 25–43.
45. Kim DY, Nishiyama Y, Wada M, Kuga S. High-yield carbonization of cellulose by sulphuric acid impregnation. Cellulose. 2001;8:29–33.

Peer-review history:
The peer review history for this paper can be accessed here:
http://www.sdiarticle4.com/review-history/62169